ATLAS EXPERIMENT

JUSTUS-LIEBIG-UNIVERSITÄT GIESSEN

Measurements of the total and inelastic *pp* cross section with the ATLAS detector at 8 and 13 TeV

Bundesministerium für Bildung und Forschung

FSP 103 ATLAS

Motivation

- Measurements of the total and inelastic cross sections and their energy evolution probe the non-perturbative regime of QCD
- Measurements help to tune the generators
- Important for projections of the pile-up conditions at the HL-LHC
- Provides constraints on forward particle production in cosmic air showers

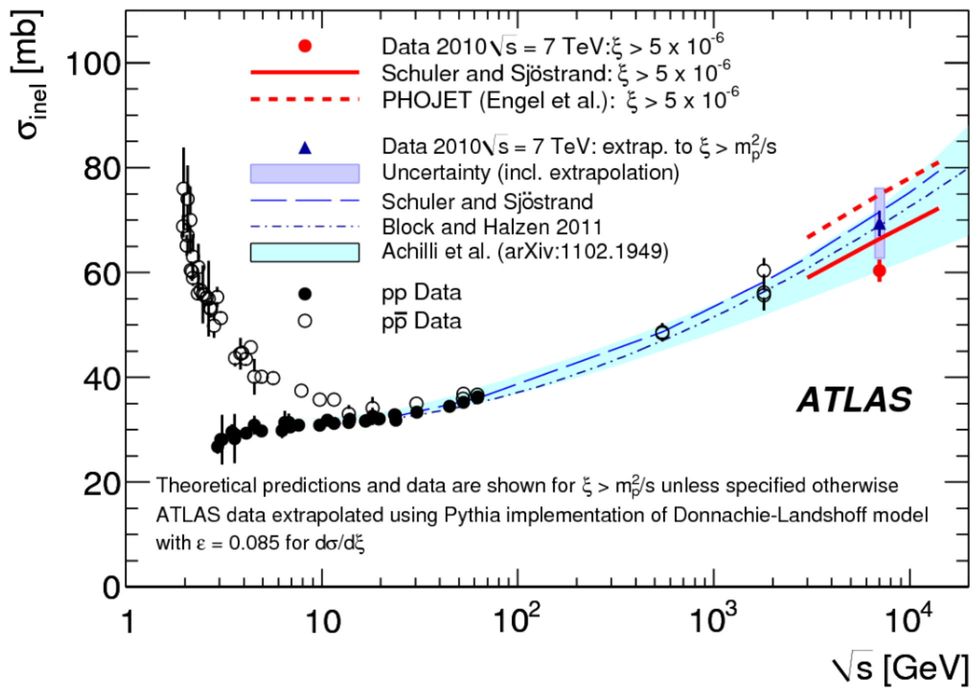

Measurement of the inelastic cross section at √s= 7 TeV
[***Nature Commun. 2 (2011) 463***]()

New measurements at 8 TeV and 13 TeV

ATLAS has performed a first series of measurements at 7 TeV where the basic methods were developed. Here the emphasis is on the new measurements recently released for publication:

Measurement of the total cross section at √s= 8 TeV **Phys. Lett. B (2016) 158**

Using the ALFA Roman Pot detector system to derive from elastic scattering and the optical theorem the total and inelastic cross section.
Special run with β*=90m at low μ≈0.1 collecting 500 /μb.

Measurement of the inelastic cross section at √s= 13 TeV **arXiv:1606.02625**

Using the MBTS forward scintillator to determine directly from the inelastic rate the cross section in the fiducial volume and extrapolated to full phase space.
Special run with at very low μ≈2.3 10^{-3} collecting 60 /μb.

Inelastic measurement with the MBTS at 13 TeV

This measurement uses the Minimum Bias Trigger Scintillator located in front of the endcap calorimeters to detect inelastic interactions. A new detector was built for run 2 with slightly larger acceptance.
Two counters of the MBTS are requested with hits above threshold to select inelastic events.

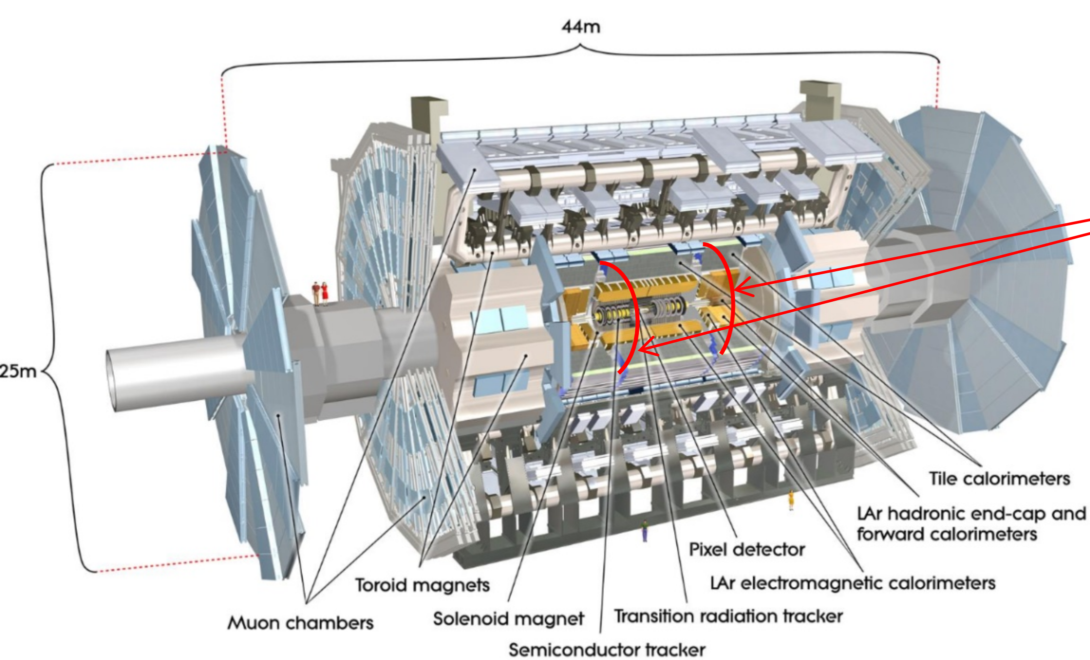

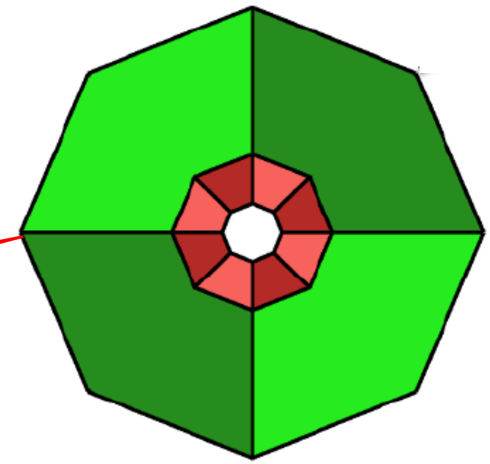

MBTS at $z=\pm 3.6$m
$2.07 < |\eta < 3.86$

The diffractive component

The fiducial volume of the measurement is determined from MC and accounts for diffractive events with a low mass of the dissociated system escaping undetected the detector.

$$M_x > 13\,\mathrm{GeV},\ \xi = \frac{M_x^2}{s} > 10^{-6}$$

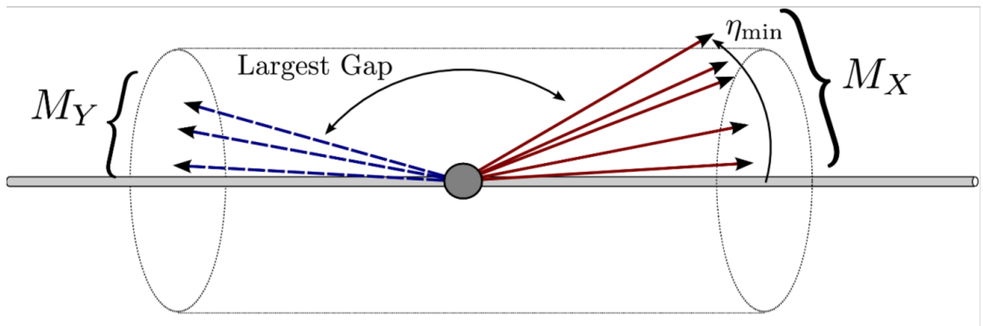

For the fiducial region the selection efficiency is above 50 %.

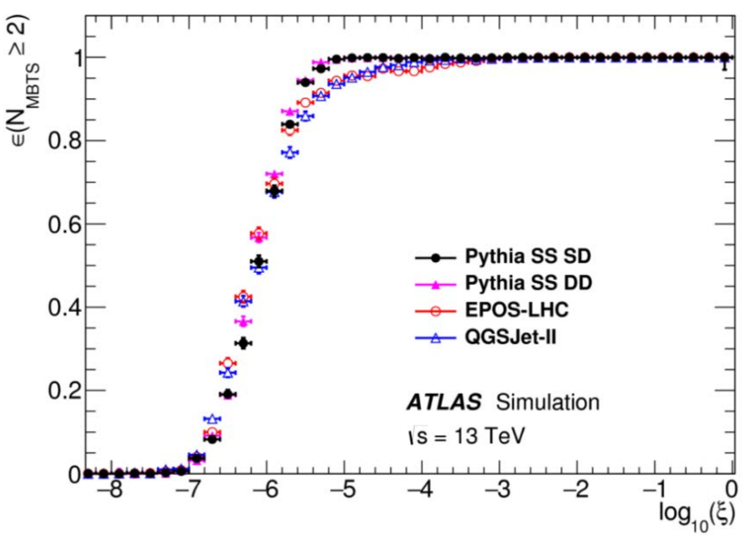

fiducial cross section

$$\sigma_{\mathrm{inel}}^{\mathrm{fid}}\left(\xi > 10^{-6}\right) = \frac{N - N_{\mathrm{BG}}}{\epsilon_{\mathrm{trig}} \times \mathcal{L}} \times \frac{1 - f_{\xi<10^{-6}}}{\epsilon_{\mathrm{sel}}}$$

N: Number of observed events
N_{BG}: Number of background events (beam-gas, beam halo, activation)
ε_{trig} : Trigger efficiency, determined using other detectors
ε_{sel} : Selection efficiency from MC, requiring two MBTS hits
1-f_{ξ} : Migration of small ξ-events in the fiducial region
L: Luminosity

Two selections are applied which enable tuning of the simulation:

1. Inclusive sample: at least 2 MBTS hits (4.2M events)
2. Single-sided sample: at least 2 MBTS hits on one side, veto on the other side (440K events)

Model tuning

The measured value of $R_{SS} = \frac{N_{\text{single-sided}}}{N_{\text{inclusive}}} = 10.4\% \pm 0.4\%$ is used to constrain in the MC the composition of diffractive and non-diffractive processes $f_D=(\sigma_{SD}+ \sigma_{DD})/ \sigma_{inel}$

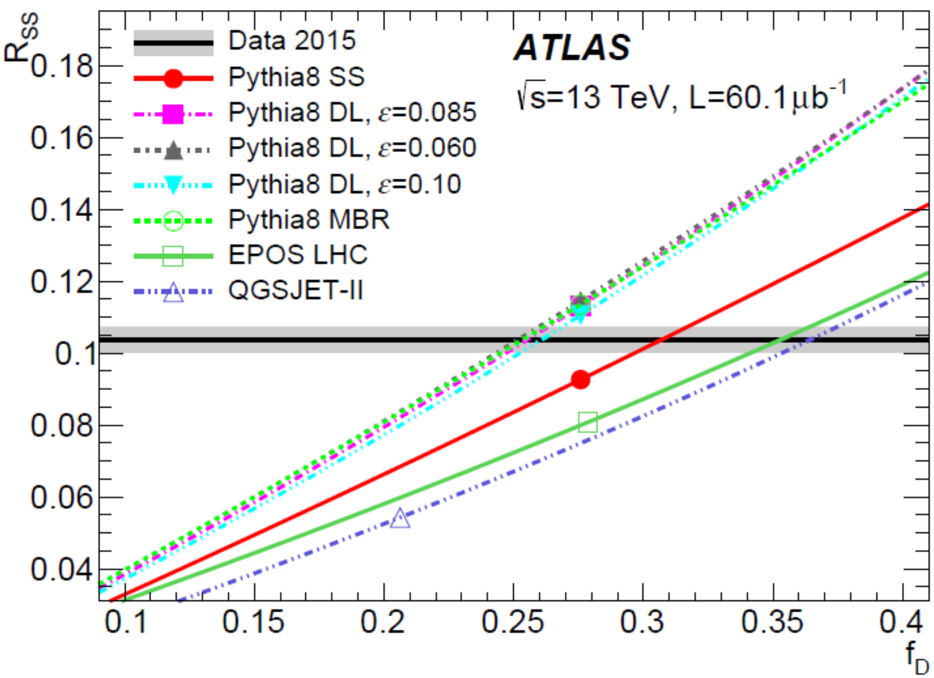

The tuned models are used to calculate ε_{sel} and $1-f_{\xi}$.

Tuned models compared to data

Background-corrected MBTS hit distributions are compared to different tuned model predictions.

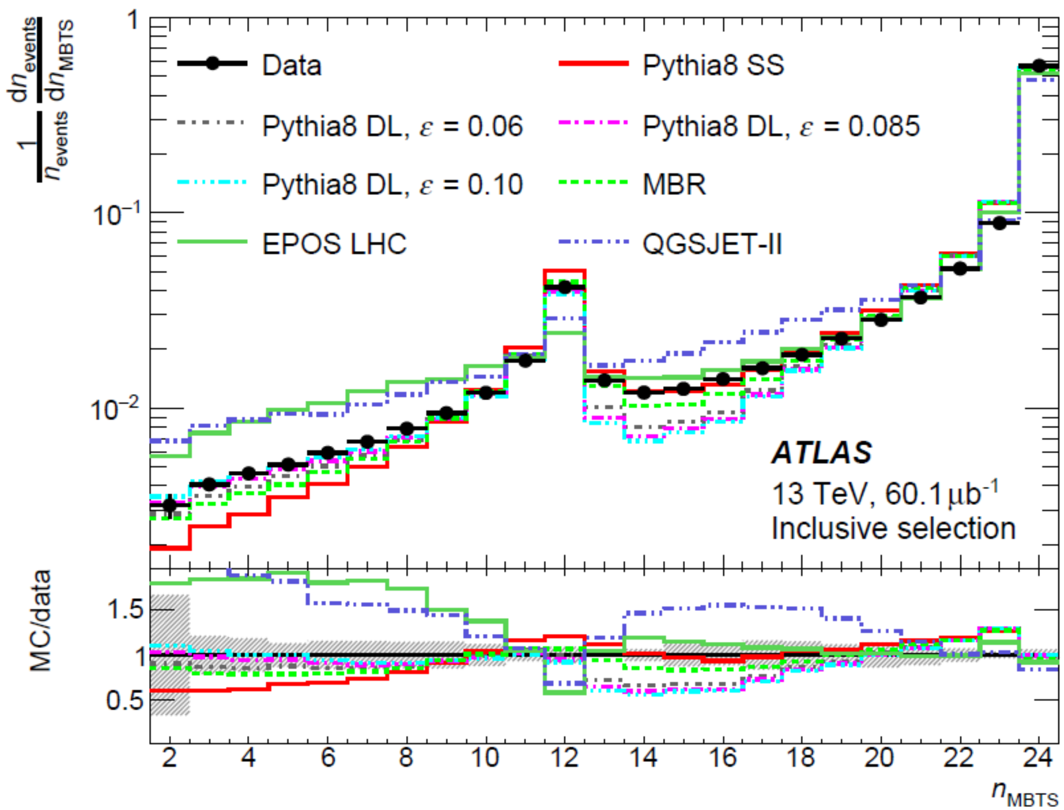

Best description is obtained for PYTHIA with the pomeron flux model from Donnachie and Landshoff with ε=0.085.
Other DL and MBR models are used for systematics. EPOS and QGSJET do not describe the data well.

fiducial cross section results

$$\sigma_{\text{inel}}^{\text{fid}}(13\,\text{TeV}) = 68.1 \pm 0.6\,(\text{exp.}) \pm 1.3\,(\text{lumi})\,\text{mb}$$

Factor	Value	Rel. uncertainty
Number of events passing the inclusive selection (N)	4159074	–
Number of background events (N_{BG})	51187	±50%
Integrated luminosity [μb^{-1}] ($\mathcal{L}$)	60.1	±1.9%
Trigger efficiency (ϵ_{trig})	99.7%	±0.3%
MC correction factor (C_{MC})	99.3%	±0.5%

Dominant uncertainty for the fiducial cross section is the luminosity.
Good agreement is observed with the PYTHIA DL models.

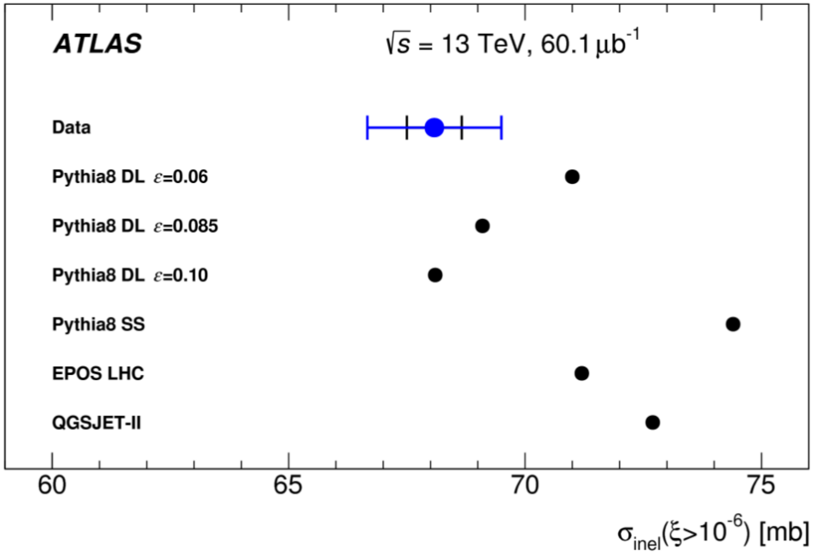

Total inelastic cross section

The extrapolation to full phase space combines previous measurements at 7 TeV with a MC-based correction:

$$\sigma_{\text{inel}} = \sigma_{\text{inel}}^{\text{fid}} + \sigma^{7\text{ TeV}}(\xi < 5\times10^{-6}) \times \frac{\sigma^{\text{MC}}(\xi < 10^{-6})}{\sigma^{7\text{ TeV, MC}}(\xi < 5\times10^{-6})}$$

where $\sigma^{7\text{ TeV}}(\xi < 5\times10^{-6})$ =11.0±2.3 is the difference between the total inelastic measurement from ALFA and fiducial measurement with the MBTS at 7 TeV.

$$\boxed{\sigma_{\text{inel}}(13\,\text{TeV}) = 79.3 \pm 0.6\,(\text{exp.}) \pm 1.3\,(\text{lumi}) \pm 2.5\,(\text{extr.})\ \text{mb}}$$

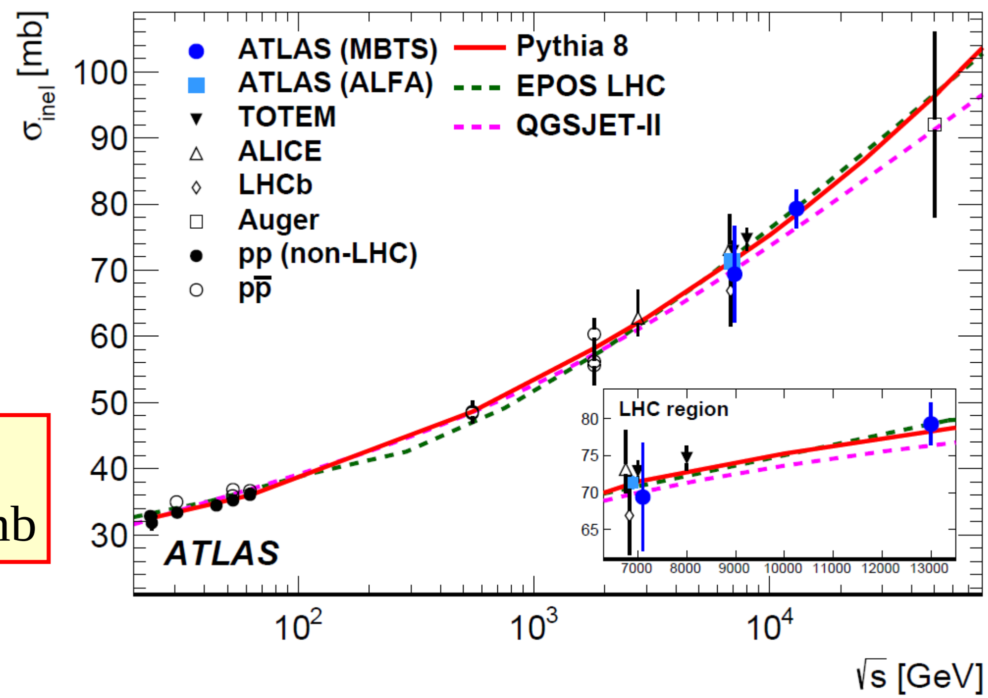

Total cross section with ALFA at 8 TeV

Measurement using the ALFA Roman Pot detector system to record elastic scattering data in a special run with high β* optics, exploiting the optical theorem : $\boxed{\sigma_{tot} = 4\pi \cdot \mathrm{Im}\left(f_{el}\right)_{t \to 0}}$

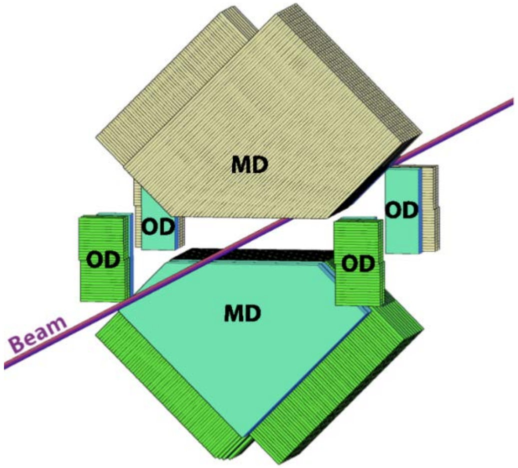

4 RP stations with vertical SciFi trackers at ~ 240m from IP 1.

The measurement principle

Measure elastic track positions at ALFA to get the scattering angle and thereby the t-spectrum dσ/dt

$$t = -\left(p\theta^*\right)^2$$

p=beam momentum, θ*=scattering angle

To calculate the scattering angle from the measured tracks

$$\begin{pmatrix} y \\ \theta_y \end{pmatrix} = \begin{pmatrix} M_{11} & M_{12} \\ M_{21} & M_{22} \end{pmatrix} \begin{pmatrix} y^* \\ \theta_y^* \end{pmatrix}$$

we need the *beam optics*, i.e. the transport matrix elements.

$$\theta_y^* = \frac{y}{M_{12}}$$

In the simplest case (high β*, phase advance 90°, parallel-to-point focusing)

EventSelection

- first level elastic trigger
- data quality cuts
- apply geometrical acceptance cuts
- apply elastic selection based on back-to-back topology and background rejection cuts

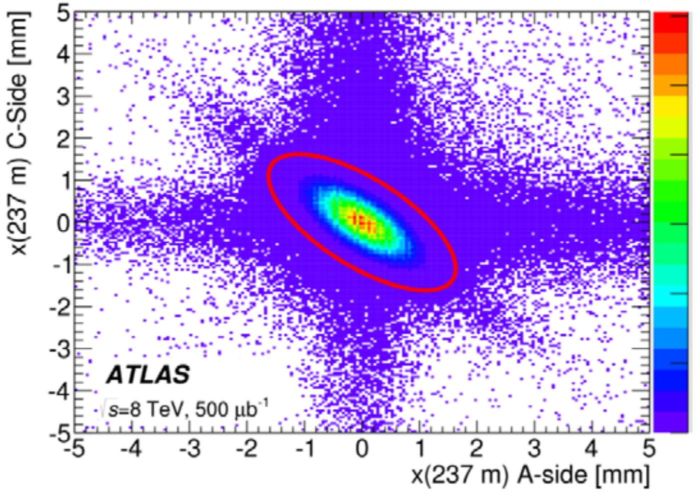

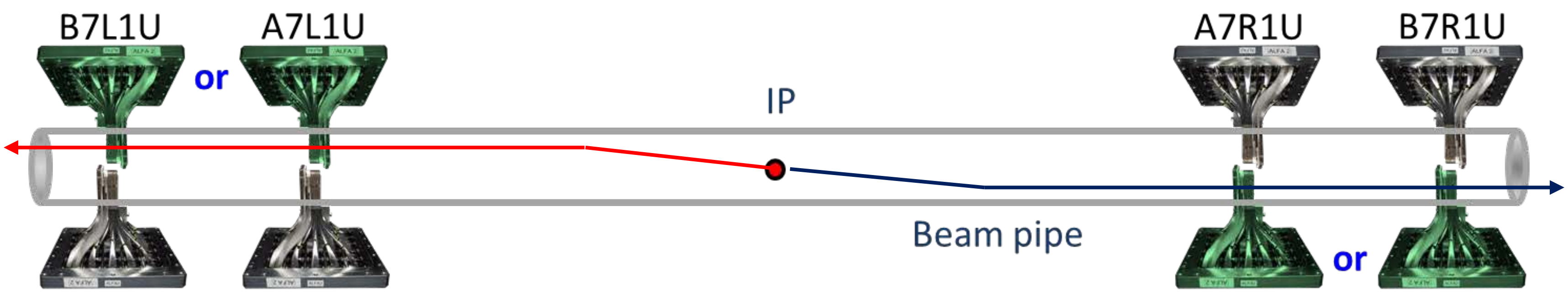

3.8 M elastics selected, background level at 0.12%, mostly DPE, subtracted.

Acceptance & unfolding

- Using PYTHIA8 as elastic scattering generator
- Matrix beam transport IP → RP (+MadX)
- Fast detector response parameterization tuned to data

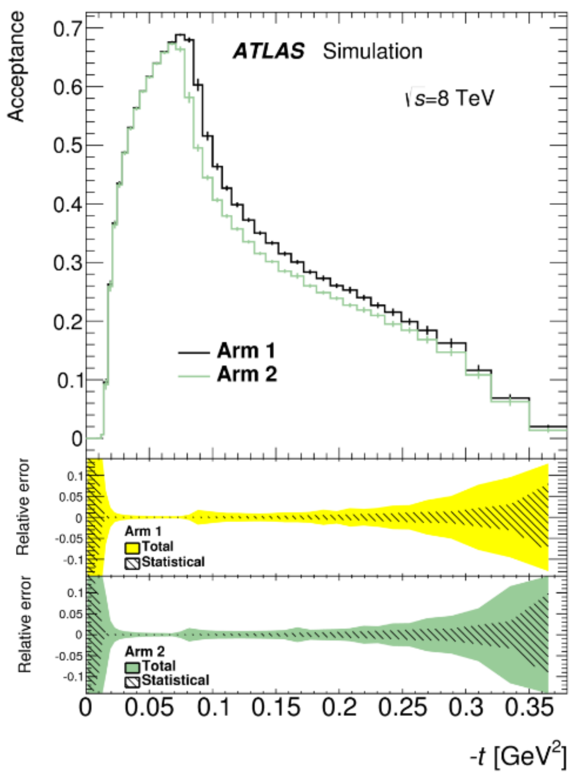

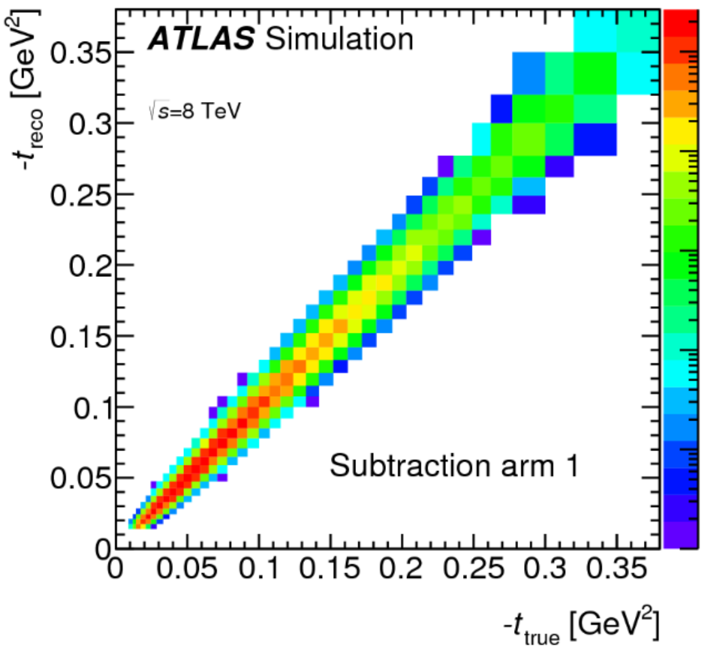

Transition matrix used as input for IDS unfolding.

Analysis of elastic data

- Data-driven method to calculate the reconstruction efficiency ~90%
- Tuning of the beam optics model with ALFA constraints → effective optics
- Trigger efficiency very high ~99.9% determined from data stream with looser conditions
- Dedicated luminosity determination resulting in a small uncertainty of only 1.5%

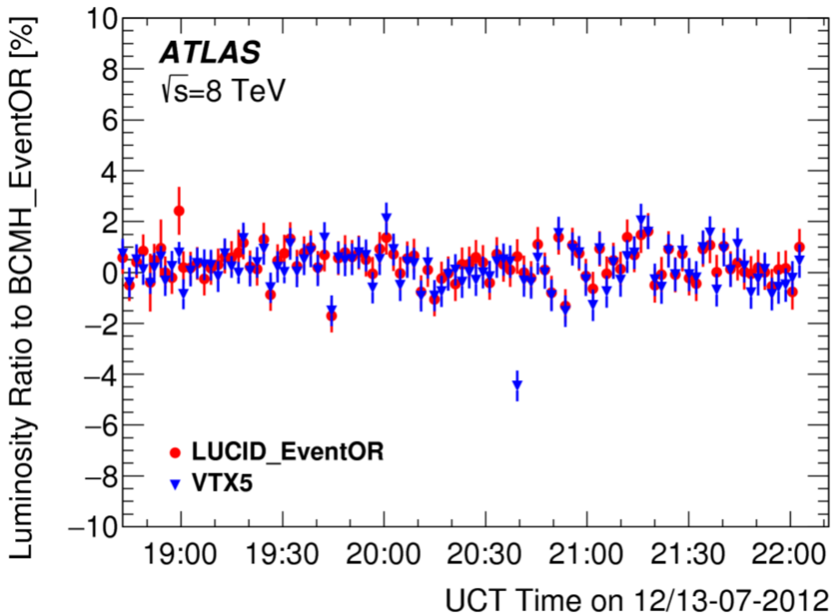

elastic cross section

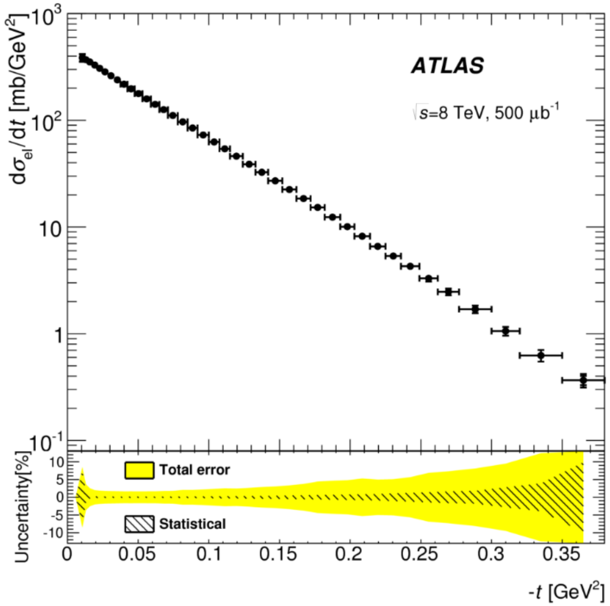

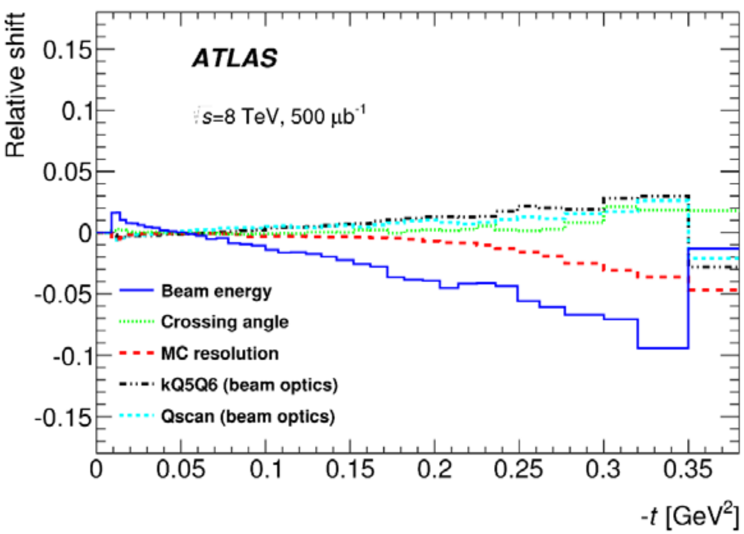

$$\left(\frac{d\sigma}{dt}\right)_i = \frac{1}{t_i} \cdot \frac{\mathrm{M}^{-1}[N_i - B_i]}{A_i \cdot \varepsilon^{reco} \cdot \varepsilon^{trig} \cdot \varepsilon^{DAQ} \cdot \mathrm{L}_{\mathrm{int}}}$$

A: acceptance(t)

M: unfolding procedure (symbolic)

N: selected events

B: estimated background

ε^{reco}: reconstruction efficiency

ε^{trig}: trigger efficiency

ε^{DAQ}: dead-time correction

L_{int}: luminosity

Main systematics:

t-independent: luminosity ± 1.5%

t-dependent: beam energy: ± 0.65%

Theoretical prediction

The theoretical prediction used to fit the elastic data consists of the Coulomb term, the Coulomb-Nuclear-Interference term and the dominant Nuclear term.

$$
\begin{aligned}
\frac{d\sigma}{dt} &= \frac{4\pi\alpha^2(\hbar c)^2}{|t|^2} \cdot G^4(t) && \boxed{\text{Coulomb}} \\
\boxed{\text{CNI}} \quad &- \sigma_{\text{tot}} \cdot \frac{\alpha G^2(t)}{|t|} [\sin(\alpha\phi(t)) + \rho\cos(\alpha\phi(t))] \cdot \exp\frac{-B|t|}{2} \\
\boxed{\text{Nuc.}} \quad &+ \sigma_{\text{tot}}^2 \frac{1+\rho^2}{16\pi(\hbar c)^2} \cdot \exp(-B|t|) \quad .
\end{aligned}
$$

ρ	0.1362
Λ	0.71 GeV^2
ϕ_C	0.577

$$G(t) = \left(\frac{\Lambda}{\Lambda + |t|}\right)^2 ,$$

Proton dipole form factor

$$\phi(t) = -\ln\frac{B|t|}{2} - \phi_C ,$$

Coulomb phase

Fit results

$$\sigma_{tot}(8\,\mathrm{TeV}) = 96.07 \pm 0.18(\mathrm{stat.}) \pm 0.85(\mathrm{exp.}) \pm 0.31(\mathrm{extr.})\ \mathrm{mb}$$
$$B(8\,\mathrm{TeV}) = 19.74 \pm 0.05(\mathrm{stat.}) \pm 0.16(\mathrm{exp.}) \pm 0.15(\mathrm{extr.})\ \mathrm{GeV}^{-2}$$

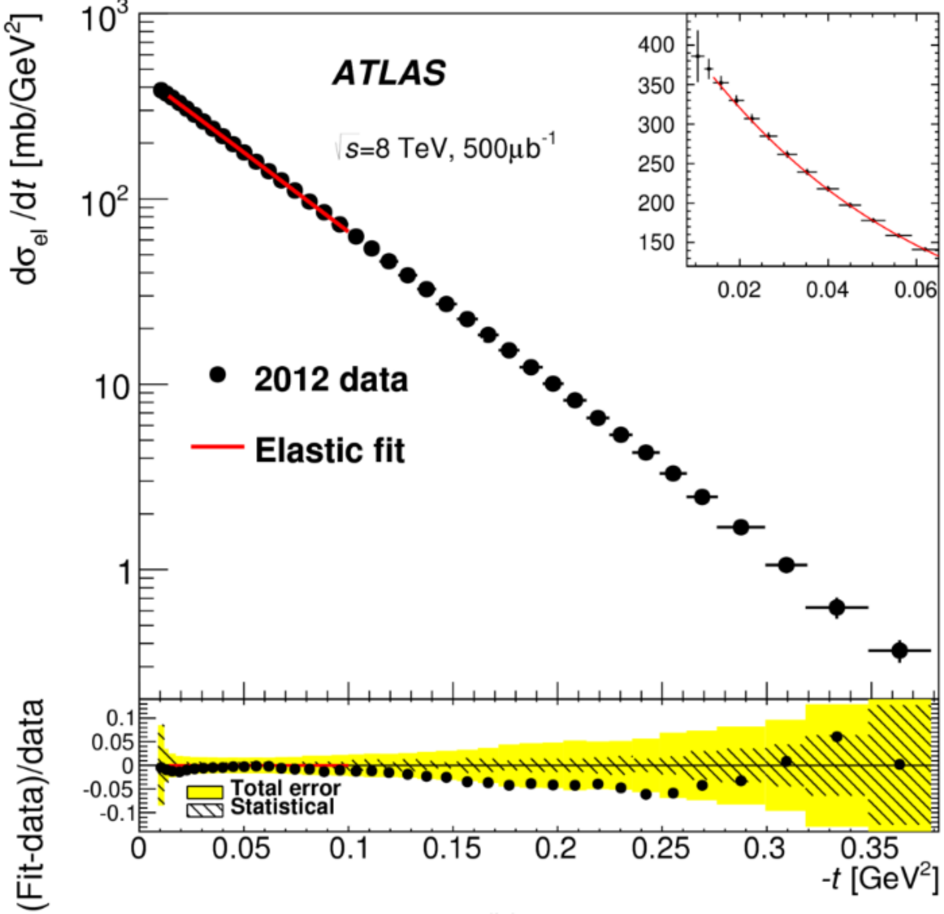

The fit includes experimental systematic uncertainties in the χ^2 (profile method).

The fit range is set to $-t[0.014,0.1]$ GeV^2, where possible deviations from exponential form of the nuclear amplitude are expected to be small.

The extrapolation uncertainty is evaluated by a variation of the fit range.

Energy evolution

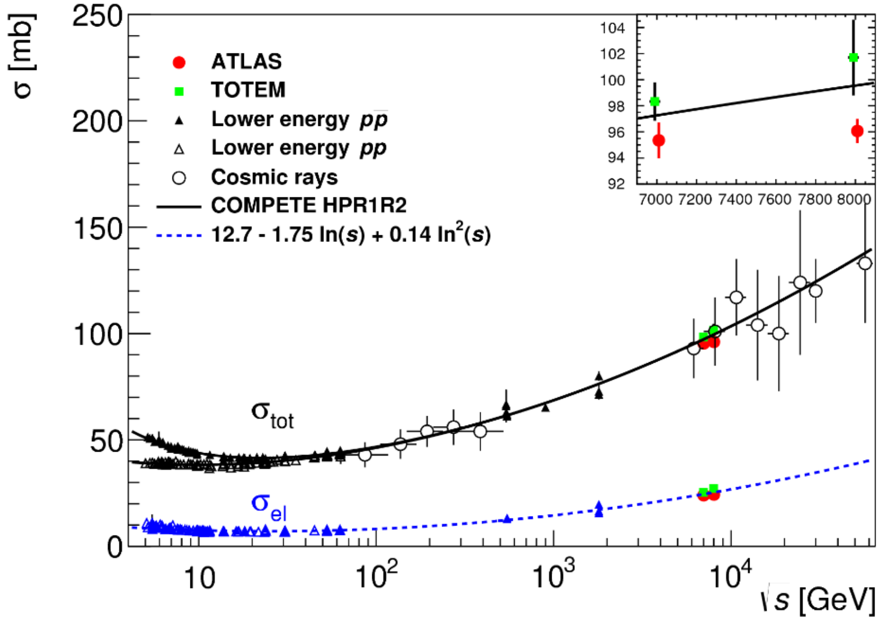

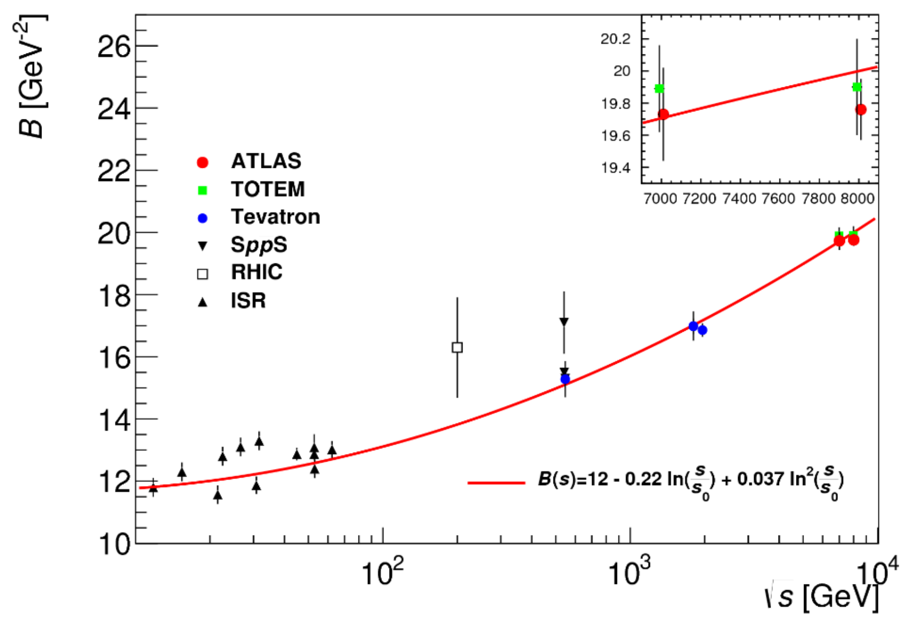

Comparison with COMPETE model [Chin. Phys. C, **38**, 090001 (2014)] for the evolution of the total cross section.

Comparison with a model from Schegelsky and Ryskin [Phys. Rev. D **85**, 094024 (2012)] for the evolution of the nuclear slope.

Derived quantities

Elastic cross section from the integrated fit-function

$$\sigma_{el} = \frac{\sigma_{tot}^2}{B} \frac{1+\rho^2}{16\pi(\hbar c)^2}$$

$$\sigma_{el}(8\,\mathrm{TeV}) = 24.33 \pm 0.04(\mathrm{stat}) \pm 0.39(\mathrm{syst})\,\mathrm{mb}$$

and inealstic cross section by subtraction $\sigma_{inel} = \sigma_{tot} - \sigma_{el}$

$$\sigma_{inel}(8\,\mathrm{TeV}) = 71.73 \pm 0.15(\mathrm{stat}) \pm 0.69(\mathrm{syst})\,\mathrm{mb}$$

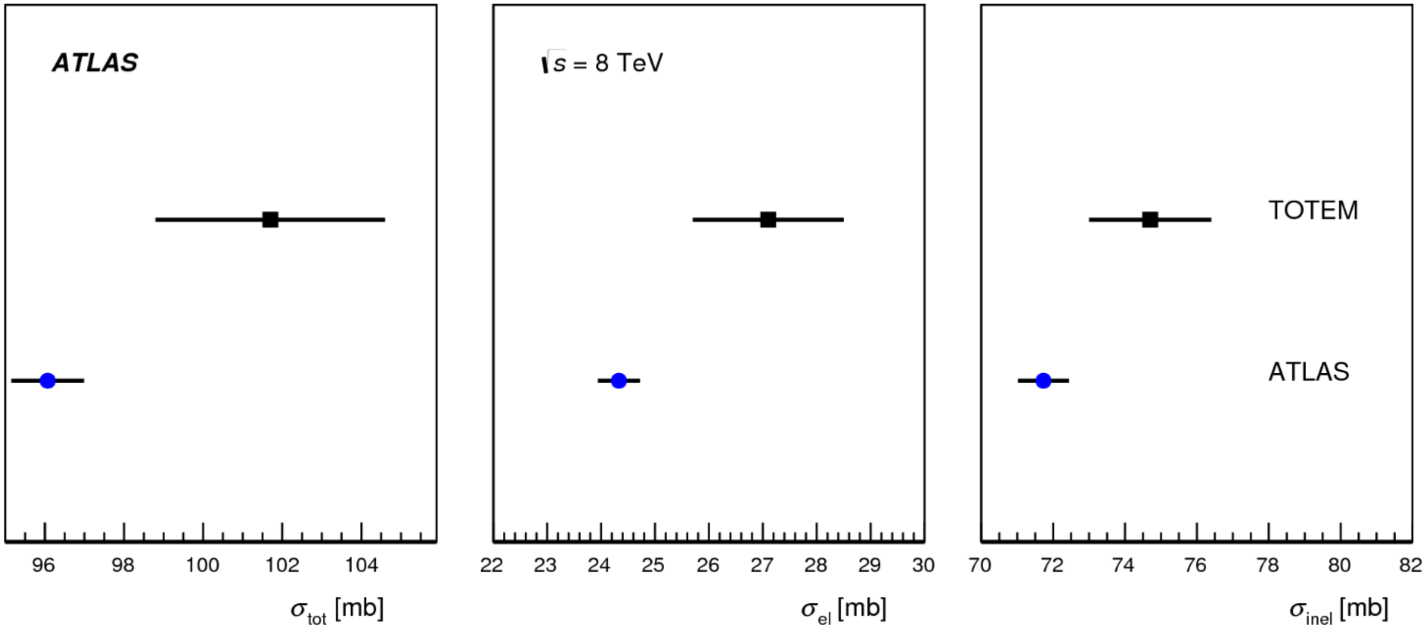

The difference between ATLAS and TOTEM is at the level of 1.9 σ, assuming uncorrelated uncertainties.

Conclusion

ATLAS has performed new measurements of inelastic cross section at 13 TeV with MBTS and of the total and inelastic cross section at 8 TeV with ALFA.

$$\boxed{\sigma_{\text{inel}}(13\,\text{TeV}) = 79.3 \pm 0.6\,(\text{exp.}) \pm 1.3\,(\text{lumi}) \pm 2.5\,(\text{extr.})\,\text{mb}}$$

$$\boxed{\begin{aligned} \sigma_{tot}(8\,\text{TeV}) &= 96.07 \pm 0.18(\text{stat.}) \pm 0.85(\text{exp.}) \pm 0.31(\text{extr.})\,\text{mb} \\ B(8\,\text{TeV}) &= 19.74 \pm 0.05(\text{stat.}) \pm 0.16(\text{exp.}) \pm 0.15(\text{extr.})\,\text{GeV}^{-2} \end{aligned}}$$

Further measurements on elastics and diffractive physics is to come with the ALFA and AFP detectors (see Mateusz and Marek‘s talks).

Back-up

Background

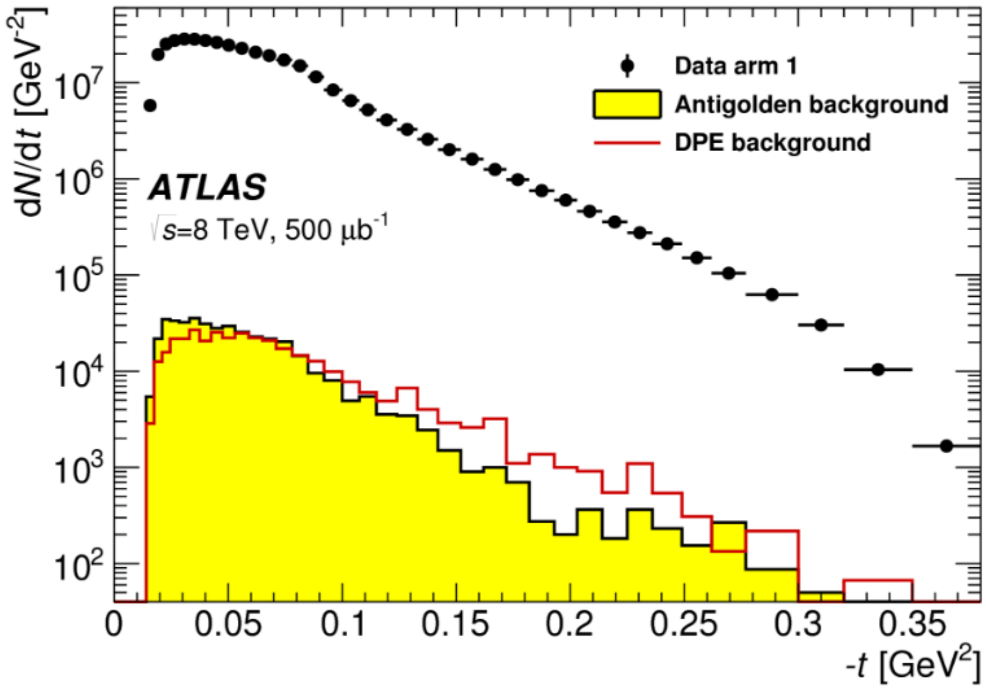

dN/dt [GeV^-2]
Data arm 1
Antigolden background
DPE background
ATLAS
√s=8 TeV, 500 μb^-1
-t [GeV^2]

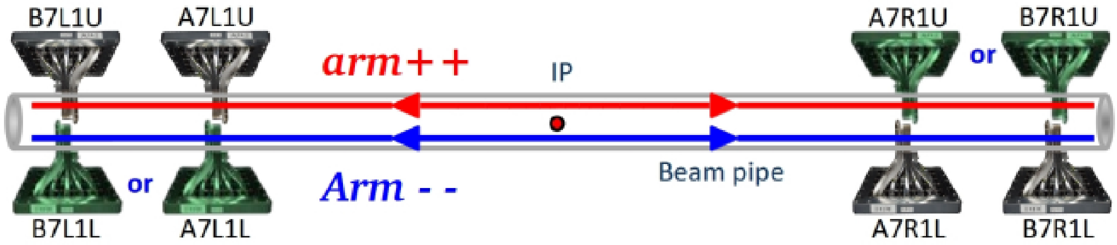

B7L1U
A7L1U
A7R1U
B7R1U
or
arm++
IP
Beam pipe
Arm - -
or
B7L1L
A7L1L
A7R1L
B7R1L

t-reconstruction methods

- subtraction method: $$\theta_u^* = \frac{u_A - u_C}{M_{12,A} + M_{12,C}}$$ $u = x, y$

- local angle method: $$\theta_x^* = \frac{\theta_{x,A} - \theta_{x,C}}{M_{22,A} + M_{22,C}}$$ y as for subtraction

- local subtraction: $$\theta_{x,S}^* = \frac{M_{11,S}^{241} \cdot x_{237,S} - M_{11,S}^{237} \cdot x_{241,S}}{M_{11,S}^{241} \cdot M_{12,S}^{237} - M_{11,S}^{237} \cdot M_{12,S}^{241}}$$ $S = A, C$

- lattice method: $$\theta_x^* = M_{12}^{-1} \cdot x + M_{22}^{-1} \cdot \theta_x$$

t-resolution

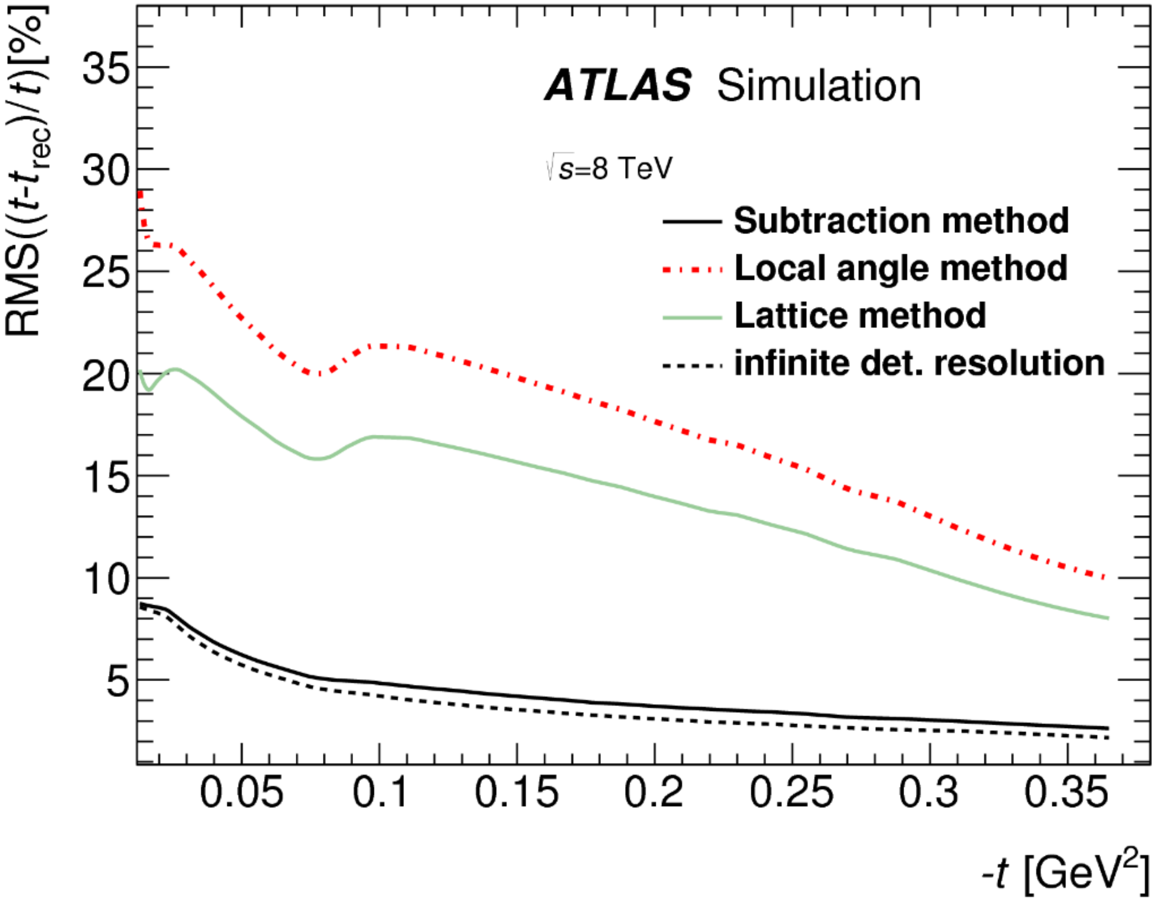

Subtraction method has by far best resolution, dominated by beam divergence.

All other methods suffer from a poor local angle resolution.

Migration

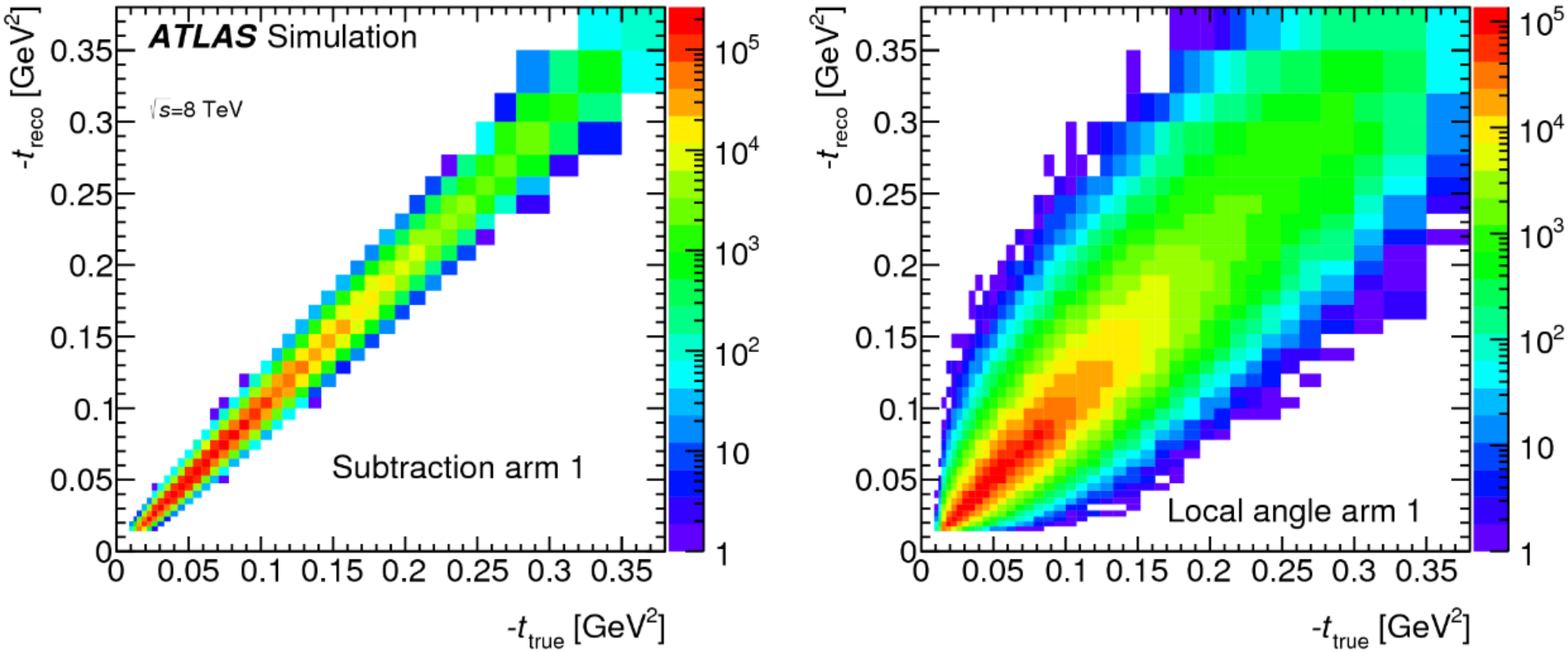

ATLAS Simulation
$\sqrt{s}$=8 TeV
Subtraction arm 1
Local angle arm 1
$-t_{reco}$ [GeV^2]
$-t_{true}$ [GeV^2]
0
0.05
0.1
0.15
0.2
0.25
0.3
0.35
1
10
10^2
10^3
10^4
10^5

Unfolding

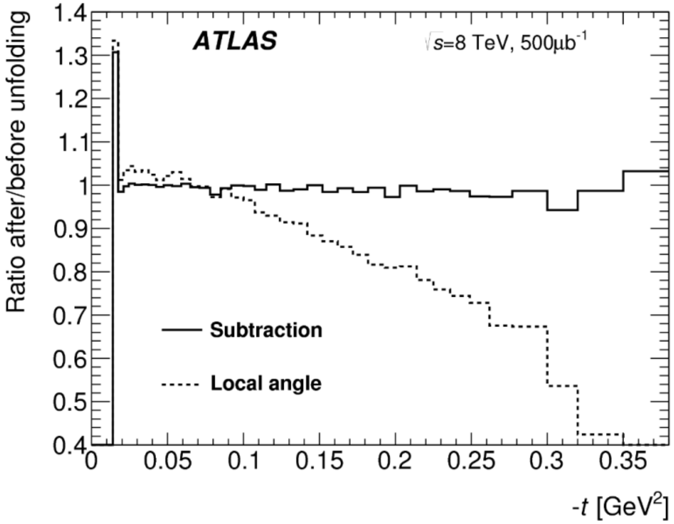

ATLAS
√s=8 TeV, 500μb-1
Ratio after/before unfolding
Subtraction
Local angle
-t [GeV2]

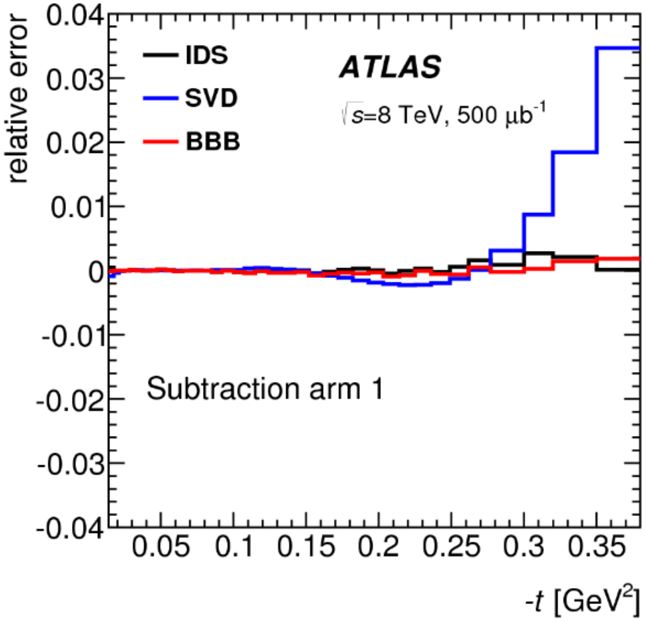

ATLAS
√s=8 TeV, 500 μb-1
relative error
IDS
SVD
BBB
Subtraction arm 1
-t [GeV2]

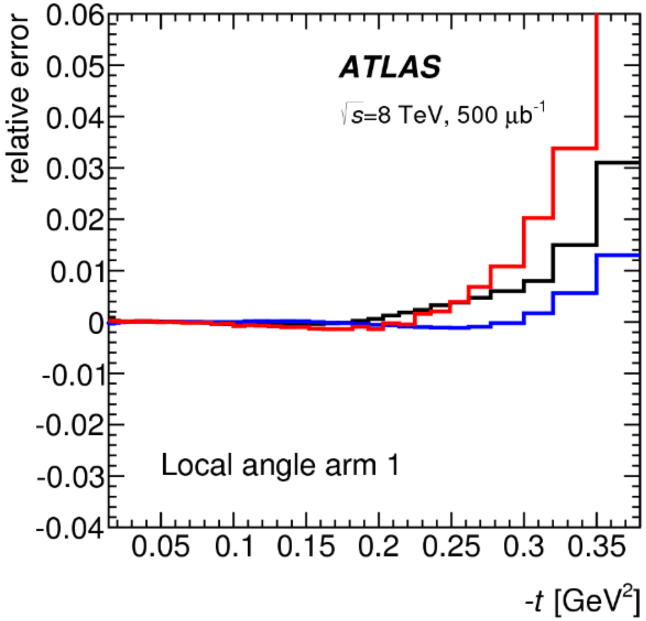

ATLAS
√s=8 TeV, 500 μb-1
relative error
Local angle arm 1
-t [GeV2]

Beam optics

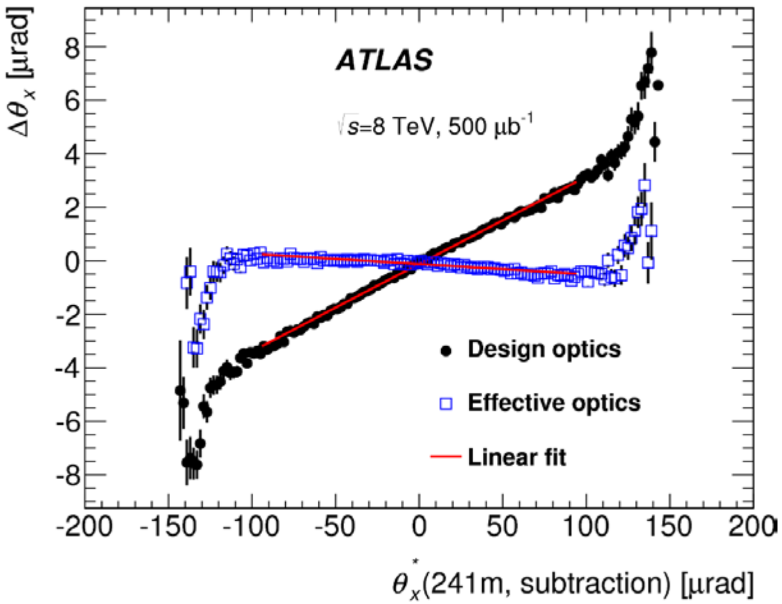
ATLAS
√s=8 TeV, 500 μb⁻¹
Design optics
Effective optics
Linear fit
Δθ*x [μrad]
θ*x(241m, subtraction) [μrad]
8
6
4
2
0
-2
-4
-6
-8
-200
-150
-100
-50
0
50
100
150
200

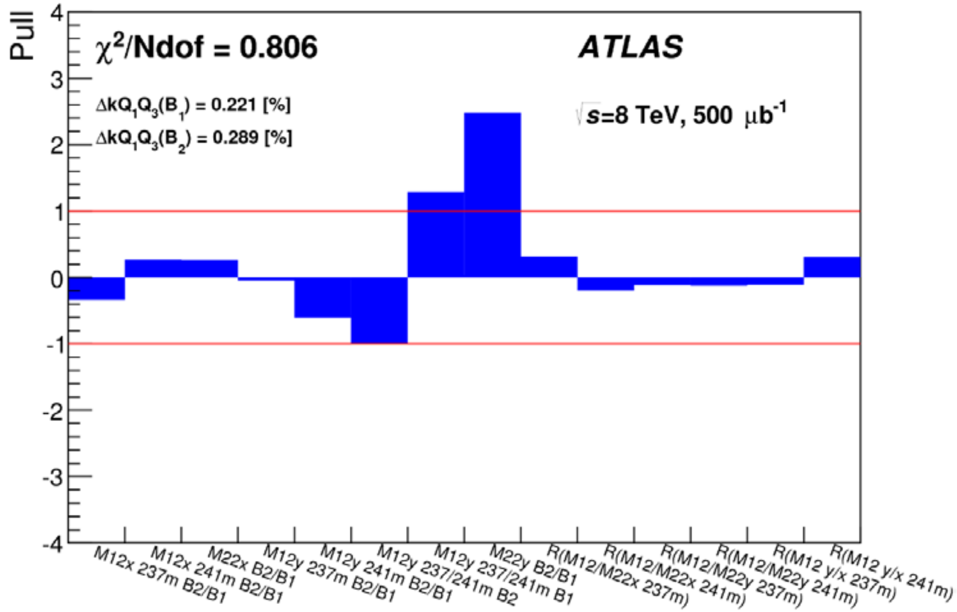
χ²/Ndof = 0.806
ATLAS
ΔkQ1Q3(B1) = 0.221 [%]
ΔkQ1Q3(B2) = 0.289 [%]
√s=8 TeV, 500 μb⁻¹
Pull
4
3
2
1
0
-1
-2
-3
-4
M12x 237m B2/B1
M12x 241m B2/B1
M22x B2/B1
M12y 237m B2/B1
M12y 241m B2/B1
M12y 237/241m B2
M12y 237/241m B1
M22y B2/B1
R(M12/M22x 237m)
R(M12/M22x 241m)
R(M12/M22y 237m)
R(M12/M22y 241m)
R(M12 y/x 237m)
R(M12 y/x 241m)

Reconstruction efficiency

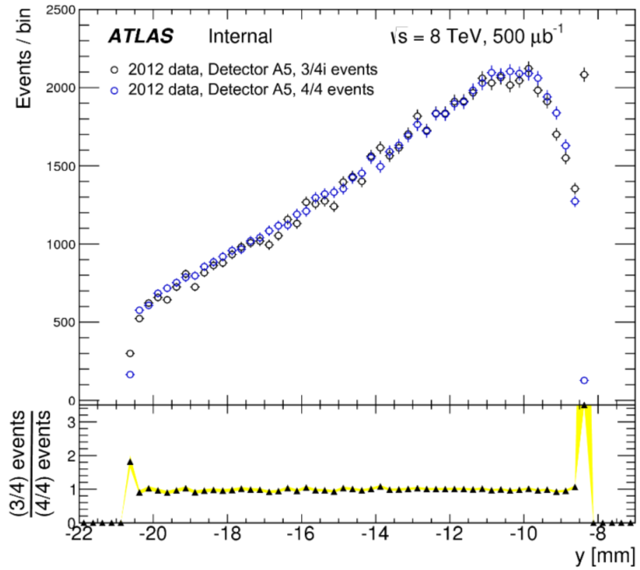

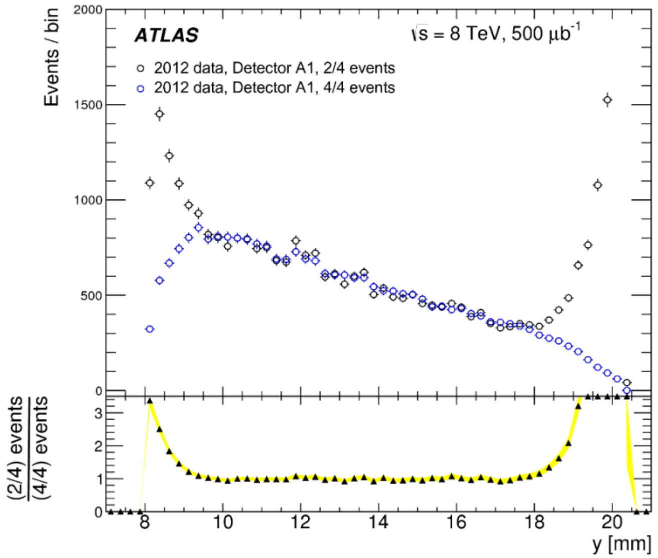

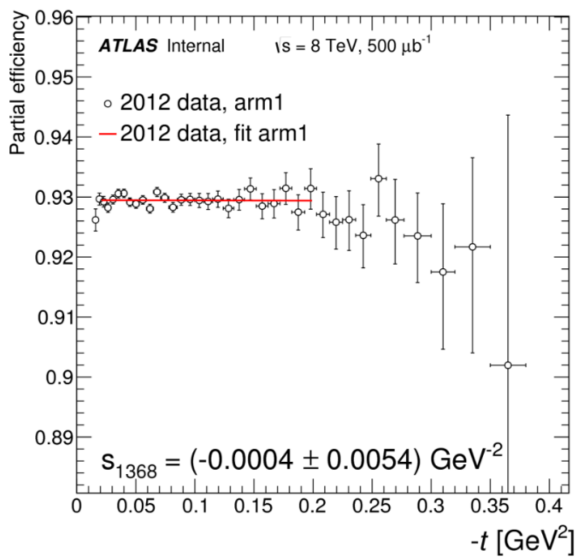

profiling method

$$\chi^2 = \sum_{i,j}\left[\left(D(i) - \left(1+\sum_l \alpha_l\right)\times T(i) - \sum_k \beta_k \times \delta_k(i)\right)\times V^{-1}(i,j)\right.$$
$$\left.\times\left(D(j) - \left(1+\sum_l \alpha_l\right)\times T(j) - \sum_k \beta_k \times \delta_k(j)\right)\right] + \sum_k \beta_k^2 + \sum_l \frac{\alpha_l^2}{\epsilon_l^2}$$

D: data, T: theoretical prediction
V: statistical covariance matrix
δ: systematic shift k in t spectrum
β: nuisance parameter for syst. shift k
ε: t-independent normalization uncertainty (luminosity, reco efficiency)
α: nuisance parameter for normalization uncertainties

ATLAS fitted nuisance parameters

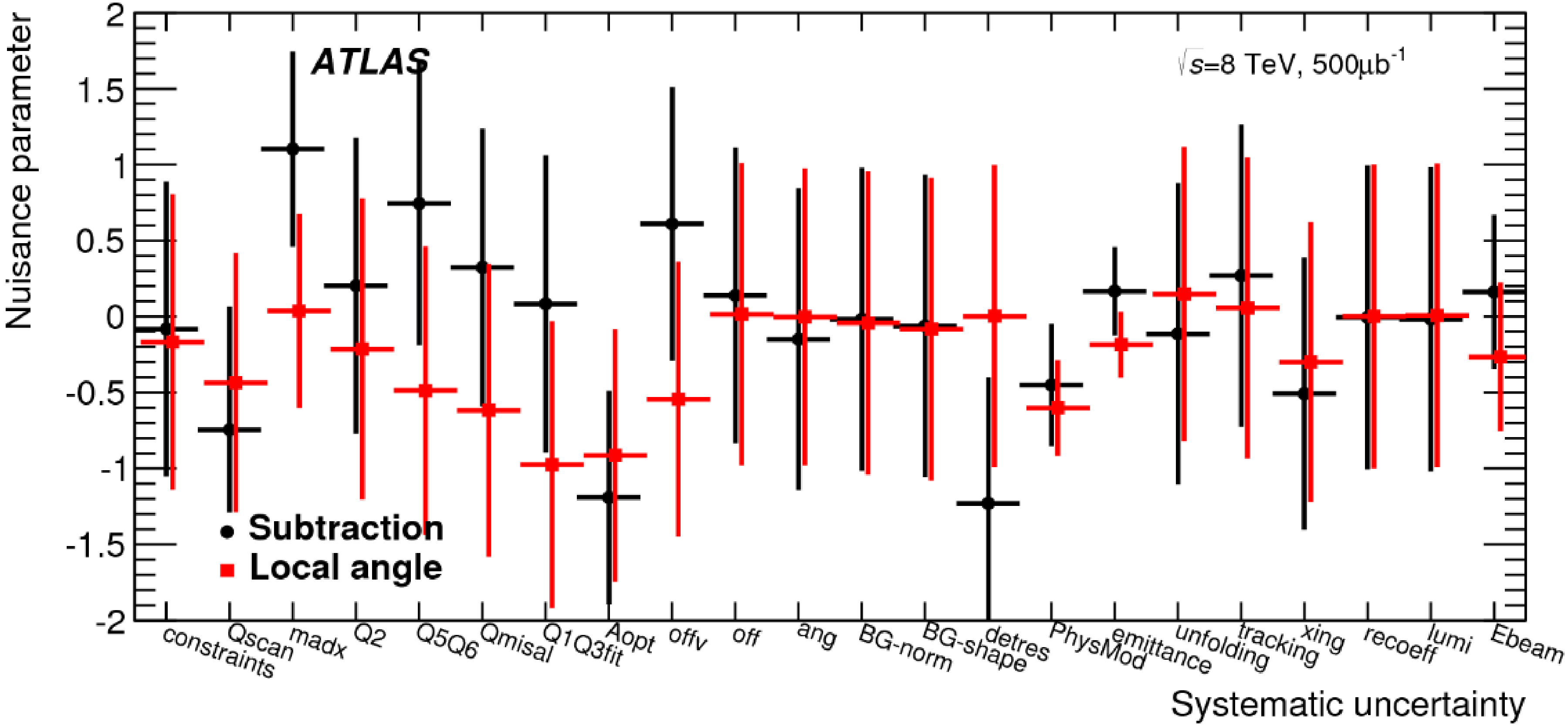

Expect nuisance parameters with mean of zero and sigma of one

Results for 4 different methods

	σ_{tot} [mb]			
	Subtraction	Local angle	Lattice	Local subtraction
Total cross section	96.07	96.52	96.56	96.58
Statistical error	0.18	0.15	0.16	0.15
Experimental error	0.85	0.94	0.88	0.89
Extrapolation error	0.31	0.42	0.23	0.23
Total error	0.92	0.98	0.93	0.93

	B $[GeV^{-2}]$			
	Subtraction	Local angle	Lattice	Local subtraction
Nuclear slope	19.74	19.83	19.87	19.88
Statistical error	0.05	0.05	0.05	0.04
Experimental error	0.16	0.18	0.16	0.17
Extrapolation error	0.15	0.17	0.14	0.15
Total error	0.23	0.26	0.22	0.23

Extrapolation uncertainty

- rho uncertainty ρ=0.1362±0.0034
- electric form factor: replace standard dipole by double dipole
- Coulomb phase: different parameterizations
- include also magnetic form factor in fit
- fit range variation by +/- 6 bins → main uncertainty

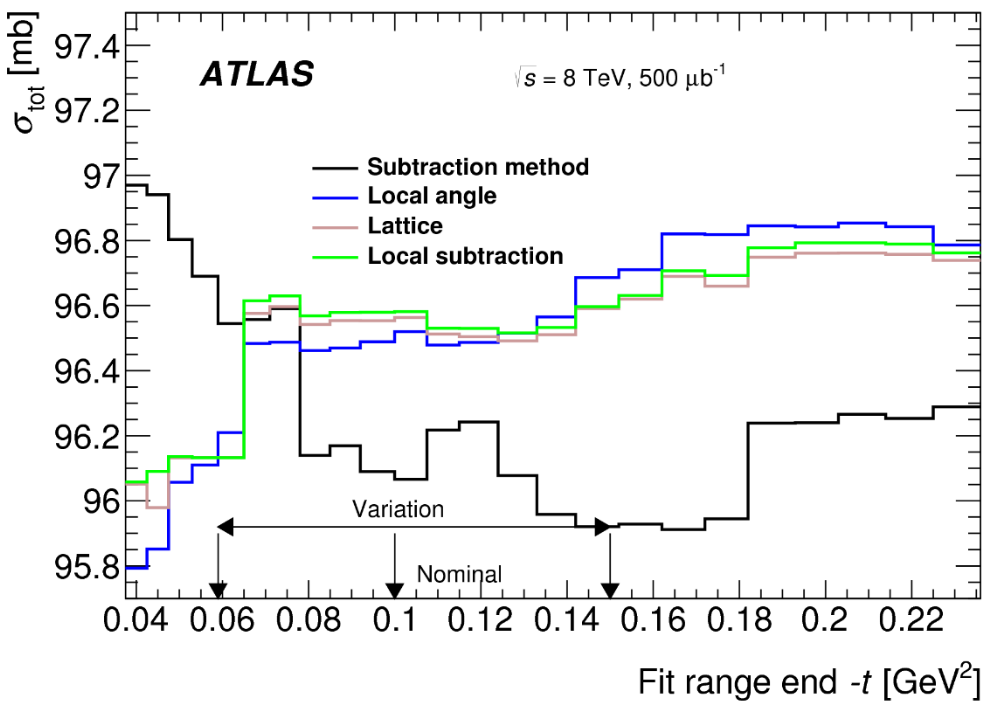

Nominal fit range 0.014-0.1 selected on the basis of theoretical arguments + acceptance> 10%

Variation up to 0.15 also theory-inspired.

Walk is typically 0.5mb sizeable difference between methods.

Alternative models

	σ_{tot}[mb]	Model
Nominal	96.07 ± 0.86	$f_{\text{N}}(t) = (\rho + i)\,\frac{\sigma_{\text{tot}}}{\hbar c} e^{-Bt/2}$
Ct^2	96.16 ± 0.80	$f_{\text{N}}(t) = (\rho + i)\,\frac{\sigma_{\text{tot}}}{\hbar c} e^{-Bt/2 - Ct^2/2}$
$c\sqrt{-t}$	96.40 ± 0.80	$f_{\text{N}}(t) = (\rho + i)\,\frac{\sigma_{\text{tot}}}{\hbar c} e^{-Bt/2 - c/2(\sqrt{4\mu^2 - t} - 2\mu)}$, $\mu = m_\pi$
SVM	96.16 ± 0.80	$f_{\text{N}}(t) = \rho \frac{\sigma_{\text{tot}}}{\hbar c} e^{-B_R t/2} + i \frac{\sigma_{\text{tot}}}{\hbar c} e^{-B_I t/2}$
BP	96.81 ± 0.95	$f_{\text{el}}(t) = i\left[G^2(t)\sqrt{A}e^{-Bt/2} + e^{i\phi}\sqrt{C}e^{-Dt/2}\right]$
BSW	96.67 ± 0.99	$\text{Re} f_{\text{el}}(t) = c_1(t_1 + t)e^{-b_1 t/2}$, $\text{Im} f_{\text{el}}(t) = c_2(t_2 + t)e^{-b_1 t/2}$

RMS from models: 0.28 mb

Stability checks

Consistency between arms

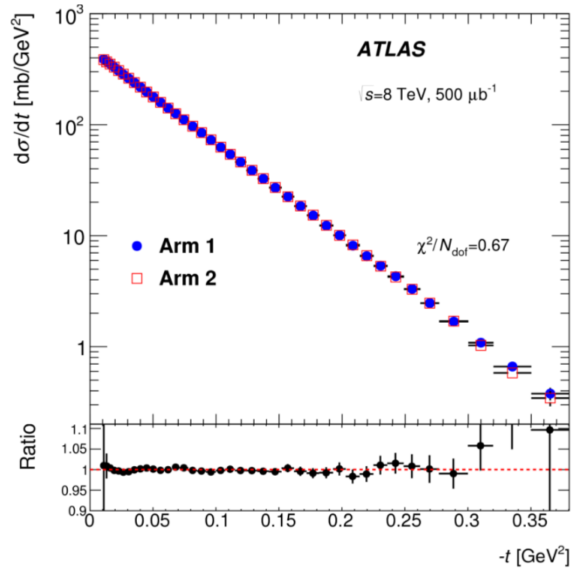

time stability

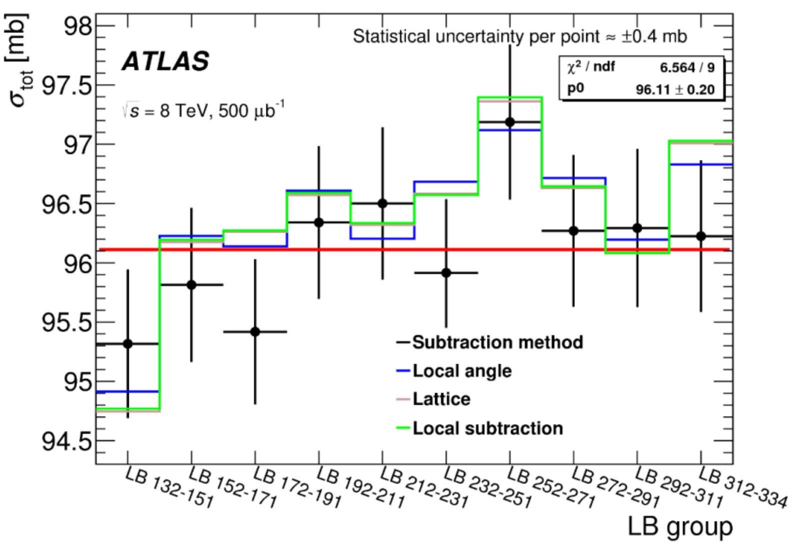

Bunch stability